Experimental Determination of Stress Fields near Notches by Reflection Photoelasticity

P. Frankovský [1,a], F. Trebuňa [1], O. Ostertag [1], F. Šimčák [1], I. Delyová [1], J. Kostka [1]

[1] *Technical University of Košice, Faculty of Mechanical Engineering, Košice, Slovakia*
[a] *peter.frankovsky@tuke.sk*

Abstract: The paper aims at the analysis of stress fields which occur while applying loads to a photoelastically coated notched sample. The analysis was done by means of reflection photoelasticity using polariscope LF/Z-2 and digital video camera. On the notched sample subject to loads by eccentric tension we determined the differences of principal normal stresses in specified point at loads from 3 kN to 12 kN. In addition, we determined the value of principal normal stress at the edge of the sample during load of 12 kN which was later compared with numerical solution in programme SolidWorks. On the photoelastically coated sample we observed maximum elongation of the coating, too.

Keywords: reflection photoelasticity; isoclinic fringes; isochromatic fringes; notch; stress field.

1 Introduction

It is crucial for design engineers to have the knowledge of stress fields of loaded components, structure knots and structural systems. At the same time, it is important to identify areas of extreme stresses properly. Such knowledge enables design engineers to optimize technical, design as well as economical features of components, structure knots and structural systems. Experimental methods are therefore helpful when carrying out stress analyses. These methods can be classified as contact methods or contactless methods. The contactless group of methods includes the optical experimental method of photoelasticity which uses polarized light to analyze the stress state. This is a progressive way of stress assessment. PhotoStress is the method of reflection photoelasticity and is one of the methods which use the phenomenon of birefringence which occurs when loading an optically sensitive material on the surface of some component. This method enables us to establish a picture of a stress field as well as gradient of stresses which occur on the surface of an examined structural component. Reflection photoelasticity is especially suitable for stress analysis of real structural components. For identification of direction and magnitude of principal normal stresses we use isoclinic and isochromatic fringes [1, 2].

Compared to other experimental methods in mechanics, PhotoStress method has the following advantageous features [3, 4]:

- visual overview of stress and strain fields throughout the whole photoelastically coated surface and, in this way, the method offers information on critical stress concentrations around holes, notches and other areas of possible failures as well as information on maximum or minimum stressed areas etc.;
- universal application which enables us to determine stresses and deformations in any point of photoelastic coating applied in laboratory conditions or directly in the field;
- non-destructive impact on surface – the experiment can be carried out repeatedly with changing load parameters;
- wide range of measurements – the method enables us to measure individual parameters and determine differences and individual principal strains and stresses, residual stresses etc.

2 Specification of sample

The determination of stress fields around the notch was done by means of reflection photoelasticity method on a steel sample made of steel X70 of 12 mm. The shape, dimensions and load of the sample are depicted in Fig. 1. The sample was cut from a steel plate with photoelastic coating PS-1A [1]. The cutting technology used is called Waterjet Cutting. Steel X70 has only small volume of carbon and its bainitic microstructure secures its high toughness and ductility level.

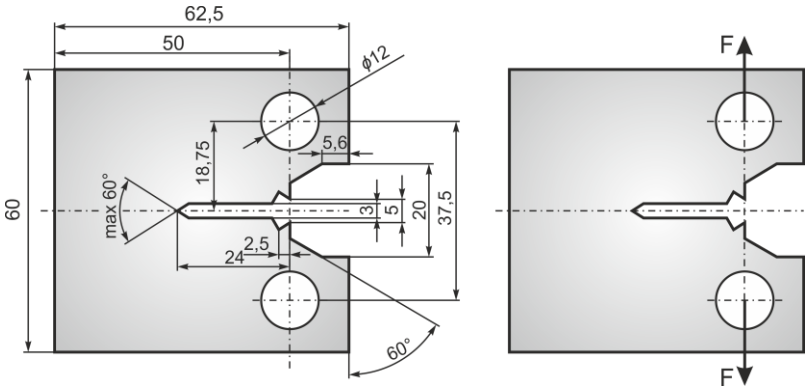

Fig. 1: Shape, dimensions and load of analyzed notched sample.

Material characteristics of the steel X70 are listed in Tab. 1 [4].

Tab. 1: Material characteristics of steel X70

Parameters	***Indication***	***Unit***	***Value***
Modulus of elasticity	E	MPa	$2.14.10^5$
Proof strength	$R_{p0.2}$	MPa	575
Proof strength	R_{eH}	MPa	586
Tensile strength	R_m	MPa	650
Elongation	A_{10}	%	24
Poisson's ratio	μ	-	0.3

Photoelastic coating PS-1A of 2.05 mm was chosen while following systematic selection methodology [9, 10]. The coating was applied to the surface of the notched sample by two-component adhesive PC-1. Photoelastic coating PS-1A is highly sensitive and hence allows us to use it in elastic as well as in elastic-plastic areas. It is delivered as a plane plate with reflective layer.

Material characteristics of the PS-1A photoelastic coating used are listed in Tab. 2 [2].

Tab. 2: Material characteristics of photoelastic coating PS-1A

Parameters	***Indication***	***Unit***	***Value***
Strain-optic coefficient	K	-	0.150
Modulus of elasticity	E	MPa	2500
Poisson’s ratio	μ	-	0.38
Elongation	A	%	5
Maximum usable temperature	t	ºC	150

Photoelastic coating applied to the analyzed notched sample (Fig. 2) transforms a part of the load and, simultaneously, strengthens the sample. As a result, deformations of the sample are lower than if no coating had been applied [5, 6].

Fig. 2: Analyzed sample with photoelastic coating.

For the above-stated purposes a correction of reinforcement effect of the photoelastic coating was done through correction coefficient for reinforcement while considering plane stress [1]

$$C_{PS} = 1 + E^* t^*, \tag{1}$$

where $E^* = \frac{E_c}{E}$ is the relation of Young's modulus of photoelastic coating and Young's modulus of the analyzed sample;

$t^* = \frac{t_c}{t}$ is the relation of coating thickness and thickness of the analyzed sample.

After calculations the value of correction coefficient, by which the order of isochromatic fringes is multiplied, is 1.0122.

3 Load specification

Experimental measurement was done on a tearing machine Zwick 1387 (Fig. 3) while loading the sample with eccentric tension. In order to fulfil the conditions of static loading the movement of the machine jaws was set to 0.5 mm/min [6].

Fig. 3: Tearing machine Zwick 1387 and reflection polariscope LF/Z-2.

Reflection polariscope LF/Z-2 with usual source of white light (Fig. 3) was used to observe isoclinic and isochromatic fringes which occur when loading the notched sample. Compensator 832 was used to read

order values of isochromatic fringes in pre-selected points. The compensator was based on the principle of null balance. Digital video camera was used to record isochromatic fringes during gradual loading of the sample.

The measurement of notch opening was done with a strain gauge and a converter (Fig. 4) which assessed the notch opening in mm [6] on the basis of electric voltage calculation. Every 1.3 s the converter registered the set of 8 000 values of electric voltage within 300 ms.

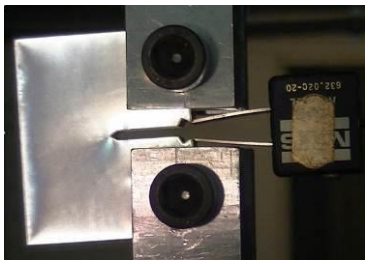

Fig. 4: Notch opening sensor.

A computer programme was written for the assessment of recorded data. The programme synchronized forces and notch openings in a time line. In order to synchronize measured data it was needed to launch the tearing machine and the converter simultaneously [6].

The relation of force F in kN to elongation f in mm was a direct outcome of the tearing machine software (Fig. 5).

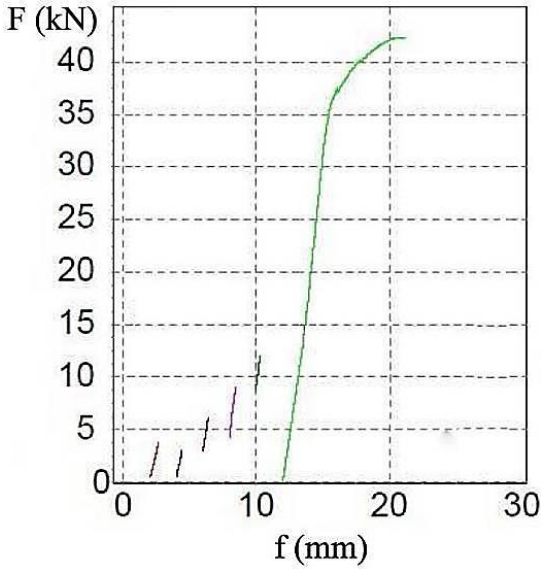

Fig. 5: Notch opening in relation to loading force.

The relation in Fig. 5 consists of a number of curves. The light green curve represents force distribution while loading the sample until crack. The notch opening increased without increasing force. The cause of this effect is that after fastening the sample in the device both surfaces had to fit firmly and adjust to each other [6]. The short curves in the initial part of the diagram (red, blue, brown, violet, dark green) represent force distributions during analysis of isoclinic and isochromatic fields while applying loads 3 kN, 4.5 kN, 6 kN, 9kN and 12 kN.

For the sample under examination were determined the following relations [6]:

- notch opening in relation to time (Fig. 6a);
- force in relation to time (Fig. 6b);
- force in relation to notch opening (Fig. 7).

Fig. 6a, Fig. 6b and Fig. 7 show us a little bounce of distribution at 38 kN. This bounce is the result of a crack in photoelastic coating.

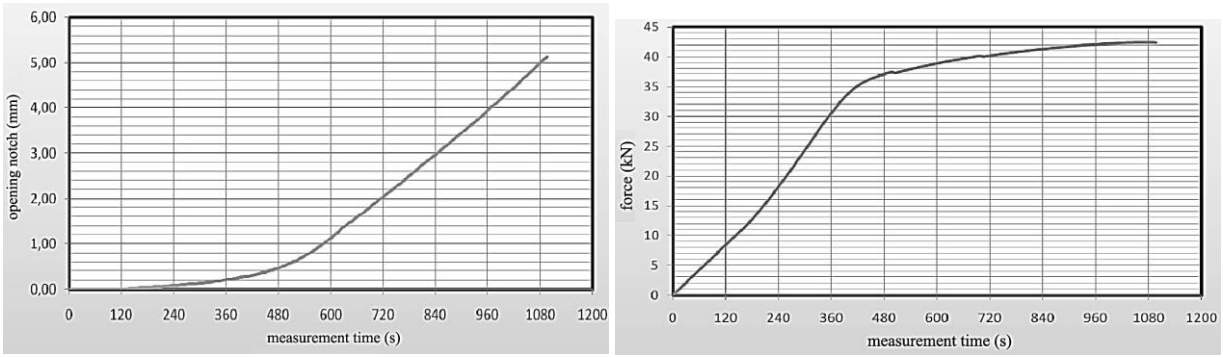

a) b)

Fig. 6: a) Notch openings in relation to time; b) Loading force in relation to time.

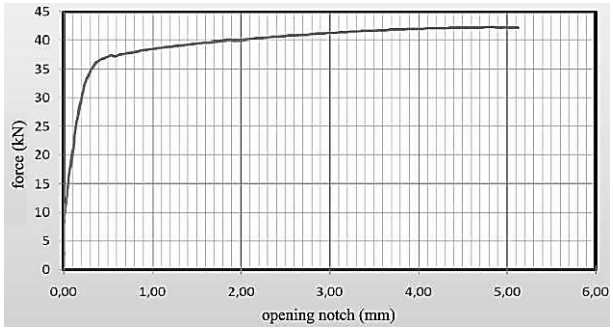

Fig. 7: Loading force in relation to notch opening.

4 Isoclinic and isochromatic fringes on the notched sample

Fig. 8 depicts isoclinic fringes on the notched sample with angle parameter α 0° to 90° and 10° increase. Isoclinic fringes were gained by reflection polariscope LF/Z-2 at plane polarized light. During examination, the analyzed notched sample was loaded by eccentric torsional force of 3 kN. Isoclinic fringes are areas in which directions of principal normal stresses are equal [6-8].

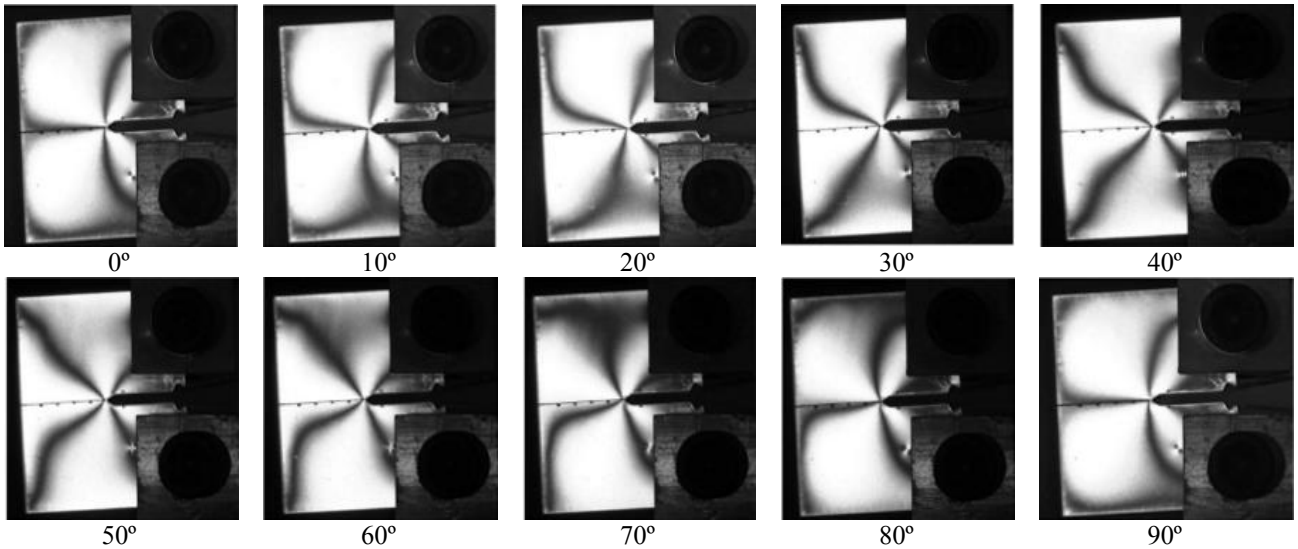

0º 10º 20º 30º 40º

50º 60º 70º 80º 90º

Fig. 8: Isoclinic fringes on the notched sample under examination.

Fig. 9 depicts isochromatic fringes during gradual loading of examined notched sample with force from 0 to 12 kN. Isoclinic fringes were observed by reflection polariscope LF/Z-2 at circularly polarized light. At loads 12 kN and higher it is possible to observe stress gradient around notch root. The high gradient is a result of high stress concentration in the point of crack occurrence [6, 9, 10].

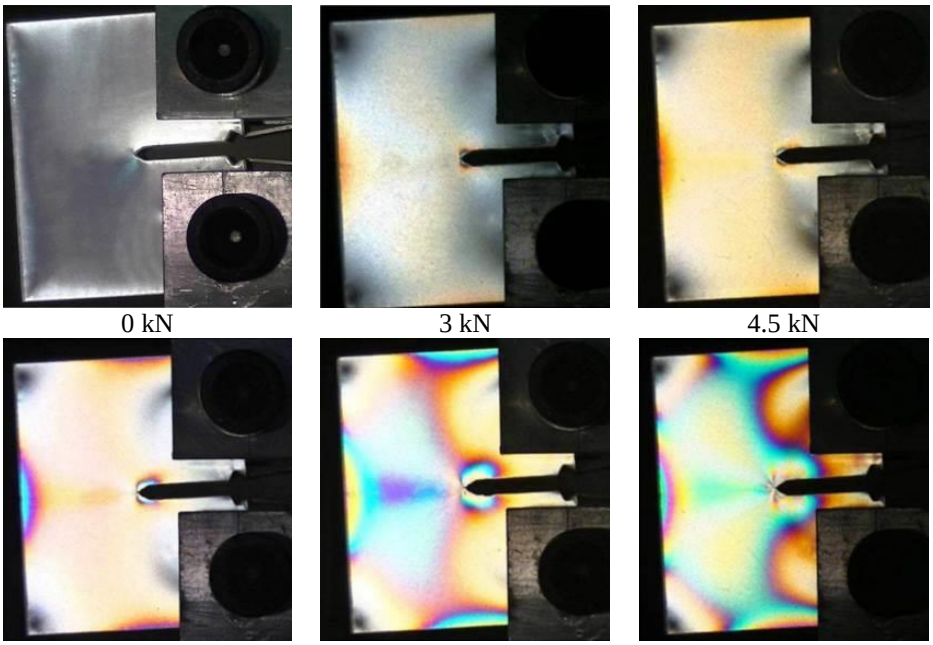

Fig. 9: Analysed sample with photoelastic coating PS-1A.

5 Principle stress analysis

Determination of principal normal stresses' difference was performed in point 1 (Fig. 10) at loading forces 3 kN, 4 kN, 6 kN, 9 kN and 12 kN.

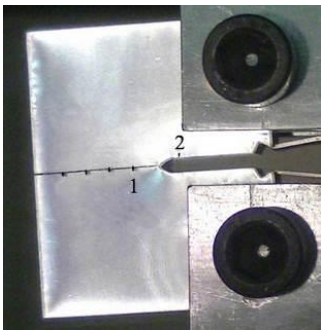

Fig. 10: Fringe order measurement points.

At the above-stated loading force values we used compensator 832 to determine the isochromatic fringe order *N*. Differences of principal normal stresses in point 1 at individual loads were determined by means of the following relation:

$$\sigma_1 - \sigma_2 = \frac{E}{1+\mu} f \cdot N, \tag{2}$$

where E is the Young's modulus of sample material, μ is Poisson's ratio of sample material and f is fringe constant of photoelastic coating.

Listed in Tab. 3 are isochromatic fringe orders *N* at point 1 under loading force f 3 kN, 4 kN, 6 kN, 9 kN and 12 kN and differences of principal normal stresses $\sigma_1 - \sigma_2$ corrected by correction coefficient *CPS* and derived from the relation (2) [1, 4].

Tab. 3: Fringe orders and difference of principal normal stresses at individual loads

Measurement	F (kN)	N (-)	$\sigma_1 - \sigma_2$ (MPa)
1	0	0	0
2	3	0.28	37.39
3	4.5	0,47	62.77
4	6	0,62	82.80
5	9	0,97	129.54
6	12	1,27	169.61

As it is known from the theoretical background, biaxial stress state requires additional measurement to determine individual values of principal normal stresses. For these purposes we use separation methods. However, there are cases when the equation (2) can be transformed to the following form:

$$\sigma_1 = \frac{E}{1+\mu} f \cdot N. \tag{3}$$

One of these cases requires free unloaded edge of an object subject to analysis. In each point of such edge we find one principal normal stress, which is non-zero tangential to the edge, and another zero normal stress. In an experimental way we used a compensator with null balance to specify the isochromatic fringe order in point 2 on the notched sample at loading force 12 kN (Fig. 10). Its value was 1.57. Using the relation (3) we subsequently determined the value of principal normal stress $\sigma_1 = 209.67$ MPa.

Numerical stress analysis was done in programme SolidWorks (Fig. 11) in order to verify previously gained value of principal normal stress σ_1 in point 2. Principal normal stress in point 2 determined by computer simulation has the value 200.2 MPa. The difference between principal normal stress σ_1 gained in an experimental way and numerically is 3.6%. As a result, we can state that the experimental measurement was relatively precise. This way of verification is easily applicable in everyday practice since the majority of structural elements include free edges [11].

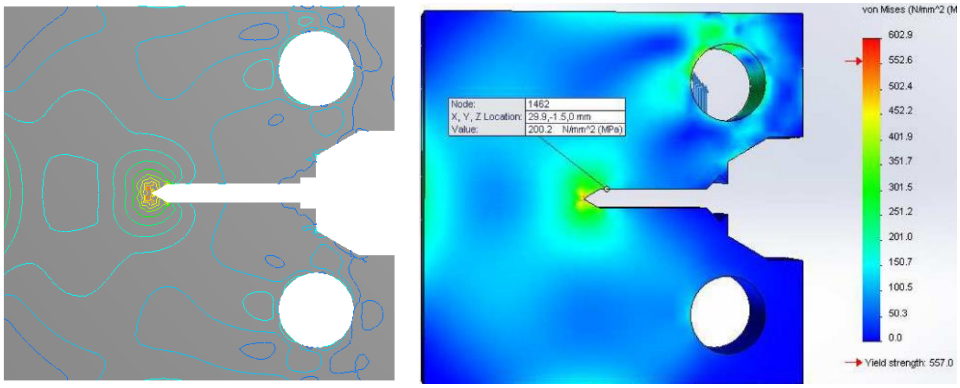

Fig. 11: Field of reduced stresses according to von Misses.

6 Verification of endurance limit of photoelastic coating

As regards tensibility of used photoelastic coating PS-1A, the manufacturer states the value of 5%. This implies that photoelastic coating is able to transform 5% of relative elongation value. Examinations were carried out on the photoelastically coated notched sample regarding the value of relative elongation at which the failure of photoelastic coating occurs [12, 13].

The failure of photoelastic coating on the notched sample occurred at loading force 38 kN and relative elongation 4% (Fig. 12). The fracture was clearly visible immediately while the crack was accompanied with sound effect [6, 14].

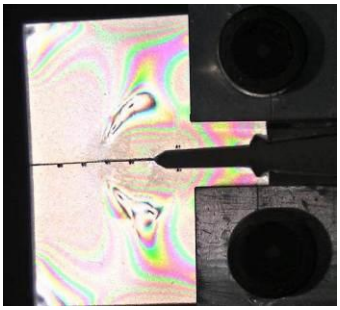

Fig. 12: Failure of photoelastic coating.

For the completeness of this issue we analysed video recording which was recorded by HD video camera and cut to individual shots of JPEG format. Fig. 13 depicts shots which are representations of characteristic moments throughout the analysis. It is obvious from Fig. 13 that stress gradient around the notch is high when the photoelastically coated sample is gradually loaded. Considering the shot No. 13 and higher it is obvious that photoelastic coating loses its ability to transform deformations and, at the same time, the ability to display isochromatic fringes. Fig. 13 no. 17 depicts the first moment when failure of photoelastic coating occurred. The shot No. 19 shows the crack spreading throughout the whole width of the sample, whereas the shot No. 20 depicts the coating peeled off under applied stresses and deformations.

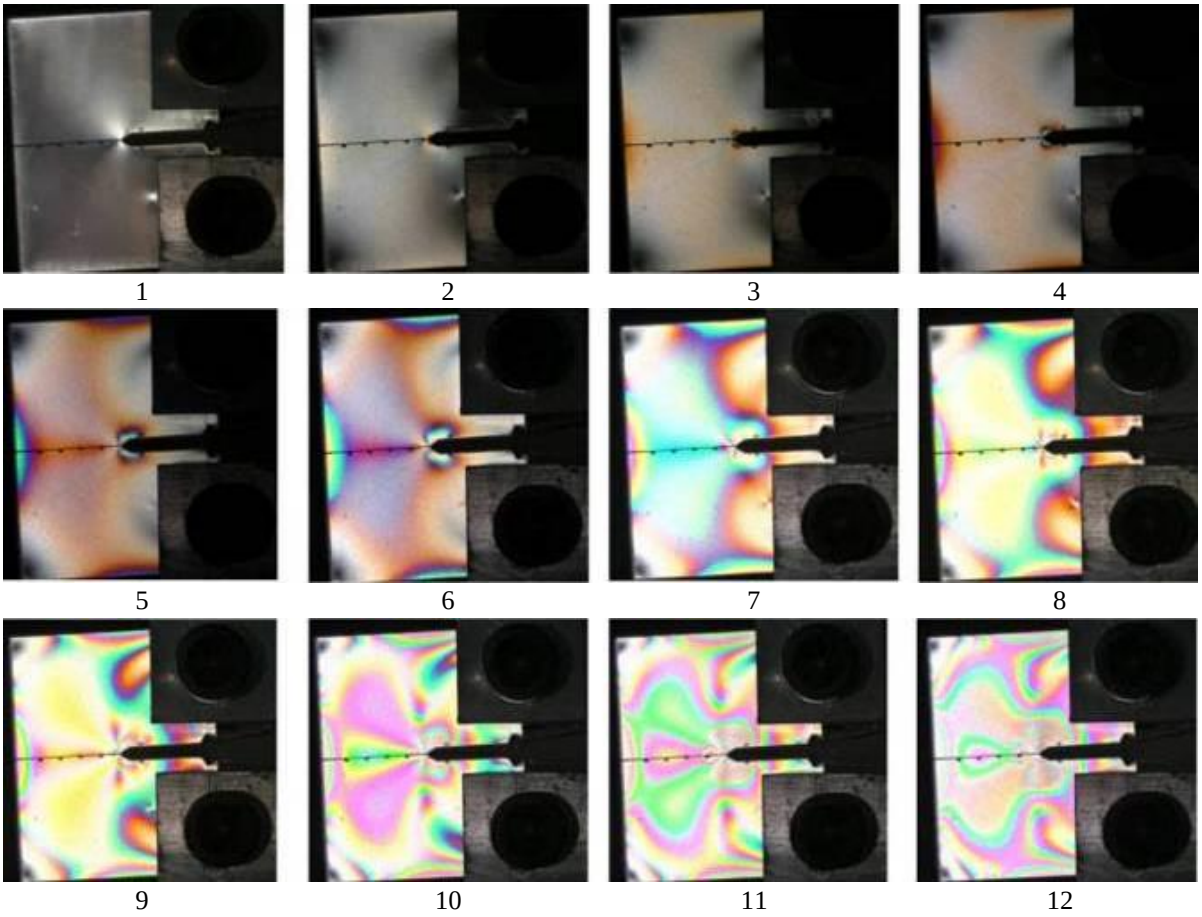

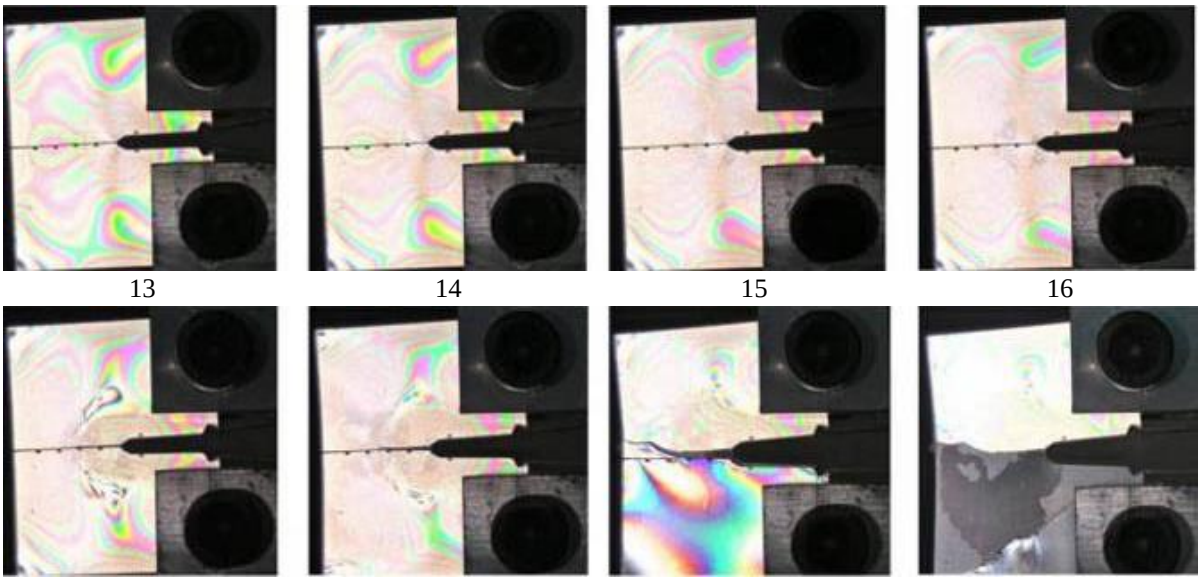

Fig. 13: Analysed sample with photoelastic coating PS-1A.

Fig. 14 depicts damaged photoelastic coating PS-1A with the notched sample and relative elongation 4%.


Fig. 14: Damaged photoelastic coating PS-1A with the notched sample and relative elongation 4%.

7 Conclusion

Using reflection photoelasticity method we were able to determine the difference of principal normal stresses in a particular point at various values of loading force. The correctness of experimentally gained data was verified through determination of one of principal normal stresses on the free edge of photoelastically coated notched sample. This measurement was verified by means of numerical simulation in programme SolidWorks. Additionally we examined the maximum elongation of the applied photoelastic coating PS-1A of the sample. The value provided by the manufacturer is 5%. Through measurements we finally determined that maximum elongation of the photoelastic coating PS-1A of 2.05 mm is 4%. This difference might have been caused by the structure of bonded joint.

Acknowledgement

This work was supported by the grand projects VEGA no. 1/0393/14, 1/0872/16 and project ITMS 26220120060.

References

[1] F. Trebuňa, F. Šimčák, Handbook of Experimental Mechanics (in Slovak), Košice, TypoPress, 2007.

[2] F. Trebuňa, J. Jadlovský, P. Frankovský, M. Pástor, Automation in the method PhotoStress (in Slovak), Košice, Technical University of Košice, 2012.

[3] A.S. Kobayashi, Handbook on Experimental Mechanics, Seattle, Society for Experimental Mechanics, 1993.

[4] M. Šmida, Using of PhotoStress method for identification of possible failures of elements in mechanical devices. Diploma thesis. TUKE, Košice, 2013.

[5] F. Trebuňa et al., The use of optical methods in experimental mechanics 2 (in Slovak), Košice, Technical University of Košice, 2015.

[6] F. Trebuňa et al., The use of optical methods in experimental mechanics 1 (in Slovak), Košice, Technical University of Košice, 2014.

[7] M. R. Ayatollahi, M. Nejati, Experimental evaluation of stress field around the sharp notches using photoelasticity. Materials & Design, 2 (2011), pp. 561-569.

[8] M. N. Pacey, M. N. James, E. A. Patterson, A new photoelastic model for studying fatigue crack closure. Experimental mechanics, 1 (2005), pp. 42-52.

[9] F. Fojtík, P., Ferfecki, Z. Paška, Computer Aided Evaluation of the Stress Tensor in the Two-Dimensional Photoelasticity, Applied Mechanics and Materials, 827 (2016), pp. 181-184.

[10] D. Post, Photoelastic stress analysis for an edge crack in a tensile field. Proc. SESA, 1 (1954), pp. 99-116.

[11] J. E. Akin, Finite element analysis concepts: via SolidWorks, 2010, World Scientific.

[12] W. B. Bradley, A. S. Kobayashi, Fracture dynamics—a photoelastic investigation. Engineering Fracture Mechanics, 3 (1971), 317-332.

[13] M. Ramulu, A. S. Kobayashi, Dynamic crack curving—a photoelastic evaluation. Experimental Mechanics, 1 (1983), pp. 1-9.

[14] C. A. Sciammarella, F. M. Sciammarella, Experimental mechanics of solids. John Wiley & Sons, 2012.